Peculiarities of $Li_{0.5}La_{0.5}TiO_3$ Formation during the Synthesis by Solid-State Reaction or Precipitation from Solutions

Anatolii Belous, Oleg Yanchevskiy, and Oleg V'yunov

V.I.Vernadskii Institute of General and Inorganic Chemistry, 32/34 Palladina Avenue, 03680 Kyiv-142 Ukraine

Odile Bohnke,* Claude Bohnke, Françoise Le Berre, and Jean-Louis Fourquet

Laboratoire des Fluorures UMR 6010 CNRS, Université du Maine, Av O. Messiaen 72085 LE MANS Cedex 9, France

Received September 5, 2003. Revised Manuscript Received November 20, 2003

It is shown that whatever the technique used, conventional solid-state reaction or precipitation from solutions, the formation of lithium lanthanum titanate, $Li_{0.5}La_{0.5}TiO_3$, is a multistage process, which occurs in a wide temperature range. Thermal analyses, X-ray powder diffraction (XRPD), and infrared (IR) spectroscopy are used to investigate the phase transformations that occur during the preparation of these ceramics. The different steps involved in the mechanism of formation of this titanate are described as temperature is increased. Both techniques lead to a pure perovskite phase. However, synthesis from solutions allows one to produce nanosized powders of titanate phase and to carry out synthesis under *milder* conditions as compared with solid state reaction synthesis. Furthermore, it has been observed that, independently of the method used, a considerable loss of lithium occurs during the synthesis of the ceramic samples and that the real composition is $Li_{0.41}La_{0.5}TiO_{2.955}$ for both ceramics. The conductivity of these ceramics has been investigated by ac impedance spectroscopy. It is shown that the ceramic samples, obtained after sintering around 1300 °C, display identical conductivity value, either for the bulk or for the grain boundary. This result is due to the close ceramic grain size obtained after sintering, as shown by scanning electron microscopy (SEM) experiments.

Introduction

Lithium-conducting materials are of great interest due to their potential use as electrolytes or electrode materials in electrochemical devices such as sensors, rechargeable batteries, miniature supercapacitors, and electrochromic displays.[1] The objects of special interest are lithium-conducting materials based on the lanthanum lithium titanate, $Li_{3x}La_{2/3-x}TiO_3$ (hereafter named LLTO), which crystallizes in perovskite-type structure (ABO_3).[2−5] The main features of lanthanum lithium titanate are its high lithium conductivity at room temperature (10^{-3} S·cm^{-1})[2−5] and its high lithium diffusion coefficient ($\sim 10^{-7}$ cm^2/s).[6] The reduction of titanium ions ($Ti^{4+} \rightarrow Ti^{3+}$) in contact with metallic lithium limits the application of lanthanum lithium titanate. This chemical reduction does not allow one to use this material directly with lithium anode for development of solid-state lithium batteries (large-scale battery systems). However, Kobayashi et al.[7] studied all-solid-state batteries based on $Li_{3x}La_{2/3-x}TiO_3$ electrolyte, where $LiMn_2O_4$ and metallic lithium were chosen as cathode and anode, respectively. To prevent the reduction of titanium, a PEO-based solid polymer electrolyte (SPE) [ethylene oxide *co*-2-(2-methoxyethoxy)ethyl ether] was sandwiched between anode (metallic lithium) and $Li_{3x}La_{2/3-x}TiO_3$. Lithium tetrafluoroborate, $LiBF_4$, was dissolved in the SPE. Such a system displayed good charge/discharge characteristics over 100 cycles at 60 °C. The possible use of such a ceramic as a pH-sensor has also been demonstrated.[8,9] This application is particularly interesting in food industry, where the use of glass electrodes is prohibited. These works[7−9] showed that these lithium-conducting perovskites, $Li_{3x}La_{2/3-x}TiO_3$, can be used in electrochemical systems due to their high conductivity at room temperature.

* Corresponding author. Tel: +33-2-4383-3354. Fax: +33-2-4383-3506. E-mail: odile.bohnke@univ-lemans.fr.

(1) West, A. R., Ed. *Solid State Chemistry and its Application*; John Willey & Sons Ltd: New York, 1994.

(2) Belous, A. G.; Butko, V. I.; Novitskaya, G. N.; Polianetskaya, S. V.; Khomenko, B. S.; Poplavko, Yu. M. *Ukr. Fiz. Zh.* **1986**, *31* (4), 576.

(3) Belous, A. G.; Novitskaya, G. N.; Polianetskaya, S. V.; Gornikov, Yu. I. *Izv. Akad. Nauk SSSR, Neorg Mater.* **1987**, *23* (3), 470.

(4) Inaguma, Y.; Liquan, C.; Itoh, M.; Nakamura, T.; Uchida, T.; Ikuta, H.; Wakihara, M. *Solid State Commun.* **1993**, *86* (10), 689.

(5) Bohnké, O.; Bohnké, Cl.; Fourquet, J.-L. *Solid State Ionics.* **1996**, *91*, 21.

(6) Birke, P.; Scharner, S.; Huggins, R. A.; Weppner, W. J. *Electrochem. Soc.* **1997**, *144* (6), L167.

(7) Kobayashi, Y.; Miyashiro, H.; Takeushi, T.; Shigemura, H.; Balakisnan, N.; Tabuchi, M.; Kageyama, H.; Iwahori. T. *Solid State Ionics* **2002**, *152/153*, 137.

(8) Bohnké, Cl.; Duroy, H.; Fourquet, J.-L. *Sens. Actuators B, Chem.* **2003**, *89* (3), 240.

(9) Bohnké, Cl.; Fourquet, J.-L. *Electrochimica Acta* **2003**, *48*, 1869.

10.1021/cm034820x CCC: $27.50
Published on Web 01/15/2004

According to the results found in the literature, it is clear that the method of synthesis affects the crystal structure and the physical properties of these titanates. Therefore, the characteristics of the above-mentioned electrochemical systems may be strongly dependent on the physical properties and consequently on the method of preparation of the ceramic. However, no data are available about the phase transformations taking place during the synthesis of lanthanum lithium titanates and how the method of synthesis affects both the formation and the electrophysical properties of LLTO. Consequently, this does not allow one to optimize the synthesis conditions of the above materials. For example, an interesting question is how to obtain fine-grained powders (nanoparticles) of lanthanum lithium titanates for application as electrode materials or sensors.

Therefore, the purpose of the present study is to investigate the phase transformations occurring during the synthesis of $Li_{0.5}La_{0.5}TiO_3$ with perovskite-like structure, either by the solid-state reaction technique or by precipitation from solutions, and to study the effect of the synthesis method on the electrophysical properties of these lithium-conducting materials.

Experimental Section

Extrapure La_2O_3, TiO_2 (rutile phase), and Li_2CO_3 were used as initial reagents for the synthesis of lanthanum lithium titanates by a solid-state reaction technique. The traces of water and adsorbed gases were removed from La_2O_3, TiO_2, and Li_2CO_3 by heat treatment during 4 h at 850, 600, and 400 °C, respectively. Reagents were weighed immediately after heat treatment and cooling of the powders in order to avoid any error in the Li:Ti and La:Ti ratios in the content of the initial powder mixture. The mixture of Li_2CO_3:La_2O_3:TiO_2 in the molar ratio 1:1:4 (suitable ratio to obtain $Li_{0.5}La_{0.5}TiO_3$) was homogenized during 6 h in a vibrating mill using corundum grinding bodies and bidistilled water. The homogenized mixture was then dried at 100 °C. Isothermal heat treatment was carried out in the temperature range from room temperature (RT) to 1300 °C during 2 h.

Aqueous solutions of extrapure $La(NO_3)_3$, $TiCl_4$, NH_4OH, and Li_2CO_3 were used as initial reagents for synthesis of lanthanum lithium titanates by precipitation from solutions. An aqueous solution of ammonia was added to a stoichiometric mixture (1:2) of solutions of lanthanum nitrate and titanium chloride. The obtained precipitates were washed, and calculated amounts of Li_2CO_3 and bidistilled water were added. Suspension after repulp washing was stripped with blending and dried at 100 °C. Dry powder was sieved through a nylon screen and isothermally heat-treated in the temperature range from 500 to 1250 °C during 2 h.

Thermal analysis was performed in a Q-1000 OD-102 device at a heating rate of 5 °C min^{-1} in air using the alundum (Al_2O_3) crucibles. The infrared (IR) spectra were recorded on a "Specord-M80" spectrometer in the 250−4000 cm^{-1} frequency range. Standards for investigation were prepared as pellets with KBr. X-ray powder diffraction experiments were carried out in a DRON-4-07 diffractometer at the room temperature using Cu Kα radiation and a step-scanning mode in the 2θ range from 10° to 90°, with a step size of 0.04°. The electrophysical properties of the ceramic samples were investigated by complex impedance spectroscopy in the frequency range from 1 Hz to 10 MHz using a 1260 frequency response analyzer and a 1296 dielectric interface from Solartron. The measurements were performed in the temperature range from 135 to 600 K under vacuum at low temperature in a cryogenerator and under dry N_2 above room temperature in an oven (Dataline). It has been verified that the electrochemical system remains linear up to 1 V (rms); therefore, the applied ac voltage was 300 mV (rms). The pellets were obtained from powders coming from either solid-state reaction or precipitation from solutions. The pellets obtained by the solid-state reaction technique were sintered for 2 h at 1300 °C and those obtained by precipitation from solutions were sintered for 2 h at 1280 °C.

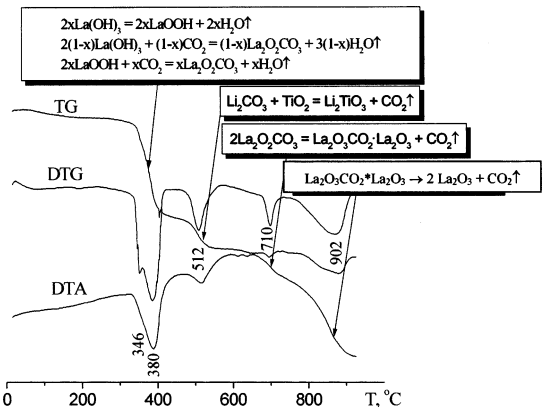

Figure 1. Results of thermal analyses of $Li_{0.5}La_{0.5}TiO_3$ samples prepared by the solid-state reaction technique.

Grain sizes of lanthanum lithium titanates obtained by precipitation from solutions before and after sintering were determined using a scanning electron microscope JEM 10CX II (JEOL). The lithium content of the perovskite-like powders was determined. To this aim a 10-fold excess of $K_2S_2O_7$ was added to fine-grained powders and alloyed during 24 h on a sand bath. The alloy was dissolved in the acidified water. The analysis of the solutions was carried out with an atomic-absorption spectrometer (SP-9 PueUnicom). Uncertainty in measurement of lithium content was not more than 2%.

Results and Discussion

(A) Phase Transformation Occurring during Preparation of Ceramics by the Solid-State Reaction Technique. It is known that the formation mechanism and the properties of end products obtained from classical solid-state reaction depend on the thermal history of the powders. In the system Li_2CO_3–La_2O_3–TiO_2, this appears to a large extent. It is explained by the fact that La_2O_3 intensively adsorbs CO_2 and H_2O from air, transforming them into carbonate and hydroxide, respectively. Li_2CO_3 also can easily adsorb H_2O. This can introduce substantial errors in the La:Ti and Li:Ti ratios on the initial stage of preparation.

Figure 1 shows the curves of thermal gravimetry (TG), differential thermal gravimetry (DTG), and differential thermal analysis (DTA) of the homogenized mixture of Li_2CO_3:La_2O_3:TiO_2 in the molar ratio 1:1:4 from room temperature to 950 °C.

Figure 2 shows the X-ray powder diffraction (XRPD) patterns and Figure 3 the IR spectra of this powder mixture as a function of heat-treatment temperature in the temperature range from 20 to 1300 °C. Both XRPD patterns and IR spectra are recorded at room temperature.

The XRPD pattern of the mixture of the initial components, after homogenization in water and drying and before any heat treatment, is shown in Figure 2 (curve 20 °C). It consists of hexagonal $La(OH)_3$ (diffraction lines A), which is formed according to reaction 1,

$$La_2O_3 + 3H_2O = 2La(OH)_3 \qquad (1)$$

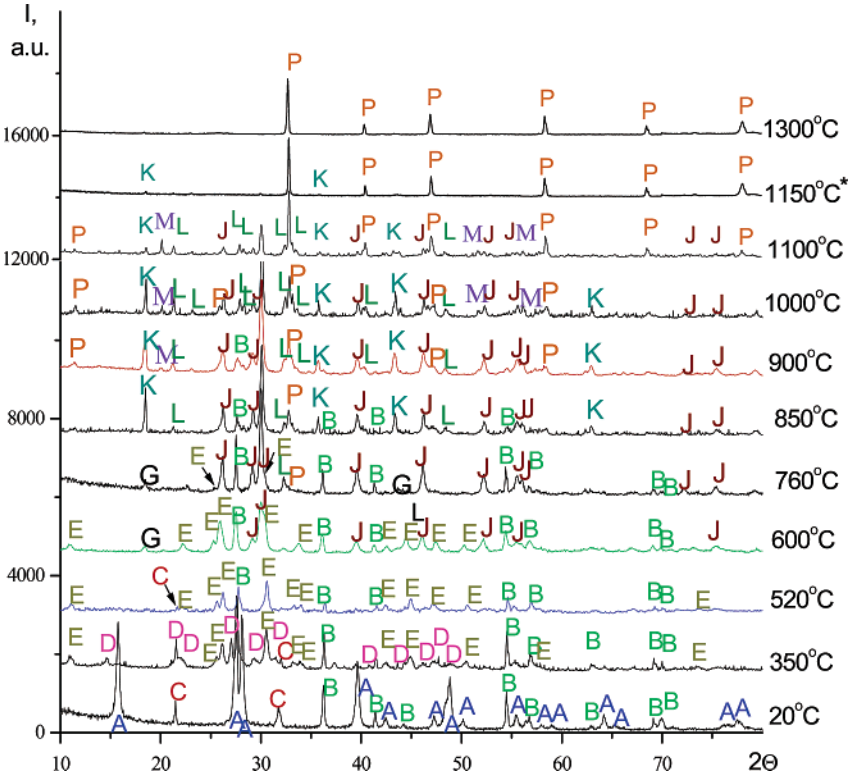

Figure 2. XRPD patterns, obtained at room temperature, of $Li_{0.5}La_{0.5}TiO_3$ samples prepared by the solid-state reaction technique after heat treatment at different temperatures. A = $La(OH)_3$ (36−1421 au); B = TiO_2 (21−1276 au); C = Li_2CO_3 (22−1141 au); D = LaOOH (19−656 au); E = $La_2O_2CO_3$ (37−804 au); G = Li_2TiO_3 (33−831 au); J = La_2O_3 (5−602 au); K = $Li_2Ti_2O_5$ (38−270 au); L = $La_2Ti_2O_7$ (28−517 au); M = $Li_2Ti_3O_7$ (34−393 au); P = perovskite LLTO.

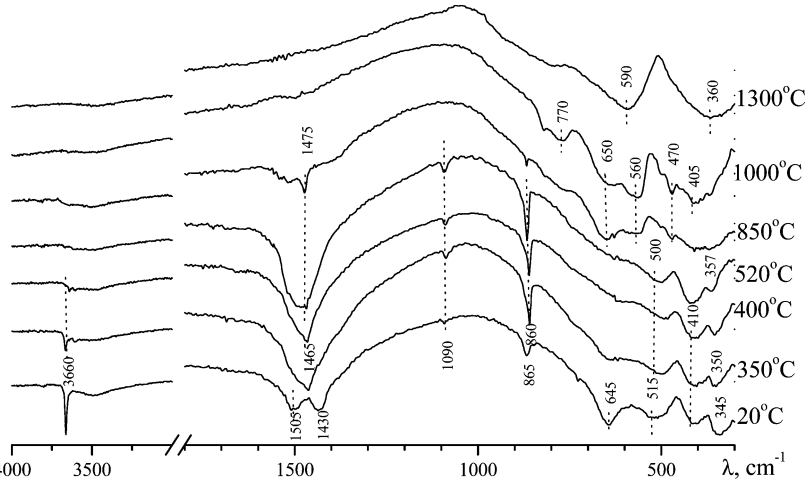

Figure 3. IR spectra of $Li_{0.5}La_{0.5}TiO_3$ powder samples prepared by the solid-state reaction technique after heat treatment at different temperatures.

tetragonal rutile TiO_2 (diffraction lines B), and monoclinic Li_2CO_3 (diffraction lines C). In addition, IR analysis shows the presence of OH groups, indicated by the narrow band of ν(OH) at ca. 3660 cm^{-1} and of δ(OH) at ca. 1090 cm^{-1} related to $La(OH)_3$ (Figure 3, 20 °C).

As heat-treatment temperature is increased, the mixture of the initial components undergo several transformations, as shown in Figure 1. At 380 °C an endothermic process is observed on the DTA curve. This is associated to a weight loss shown on the TG and DTG curves. This is due to the decomposition of $La(OH)_3$ (320−380 °C) and LaOOH (350−400 °C). These reactions are followed by the thermal decomposition of Li_2CO_3 (510−560 °C) and $La_2O_2CO_3$ (600−900 °C).

These processes are described by the following reactions (2−6):

$$2xLa(OH)_3 = 2xLaOOH + 2xH_2O\uparrow \quad 320-350\ °C \quad (2)$$

$$2(1-x)La(OH)_3 + (1-x)CO_2 = (1-x)La_2O_2CO_3 + 3(1-x)H_2O\uparrow \quad 320-380\ °C \quad (3)$$

$$2xLaOOH + xCO_2 = xLa_2O_2CO_3 + xH_2O\uparrow \quad 350-400\ °C \quad (4)$$

$$Li_2CO_3 + TiO_2 = Li_2TiO_3 + CO_2\uparrow \quad 510-560\ °C \quad (5)$$

$$La_2O_2CO_3 = La_2O_3 + CO_2\uparrow \quad 600-900\ °C \quad (6)$$

The dehydration of $La(OH)_3$ occurs in two steps in accordance with reactions 2 and 3. This fact is verified by the presence of two minima at 346 and 380 °C on the DTG curve (Figure 1). Moreover, the XRPD pattern obtained after heating the initial mixture at 350 °C (Figure 2) shows the appearance of the LaOOH (diffraction lines D) and $La_2O_2CO_3$ (diffraction lines E) phases and the disappearance of the diffraction lines A corresponding to the $La(OH)_3$ phase.

The band at 865 cm^{-1} (Figure 3, $t = 20$ °C) in the IR spectrum indicates the presence in the mixture of carbonate groups due to Li_2CO_3.[10] As the temperature increases to 350 °C, this band slightly shifts to 860 cm^{-1}. This is explained by the formation of lanthanum oxycarbonate, $La_2O_2CO_3$, which is detected by XRPD (Figure 2). This band fully disappears above 850 °C, which agrees well with the results of XRPD and thermal analysis. It should be noted that the decomposition of lanthanum oxycarbonate, $La_2O_2CO_3$ (reaction 6), occurs in two steps.[11] This conclusion is confirmed by the presence of two endothermic processes on DTG at 710 and 902 °C, which are accompanied by a considerable loss of weight. The first endothermic process at 710 °C is the first step of the lanthanum oxycarbonate decomposition according to the following reaction:

$$2La_2O_2CO_3 = La_2O_2CO_3{\cdot}La_2O_3 + CO_2\uparrow \qquad (7)$$

And the second endothermic process at 902 °C is the second step of its decomposition to finally form lanthanum oxide according to

$$La_2O_2CO_3{\cdot}La_2O_3 = 2La_2O_3 + CO_2\uparrow \qquad (8)$$

These two reactions, 7 and 8, lead to the reaction 6, as written above. These results are in good agreement with the XRPD patterns (Figure 2) that show the appearance of the La_2O_3 phase (diffraction lines J) and the concomitant disappearance of the $La_2O_2CO_3$ phase (diffraction lines E) for the mixture heat-treated up to 900 °C.

The reaction of Li_2CO_3 with TiO_2 that occurs around 510−560 °C leads to the formation of Li_2TiO_3 according to the reaction 5. This is shown by the diffraction lines G on Figure 2. This phase disappears above 820 °C to transform into the lithium dititanate $Li_2Ti_2O_5$ (diffraction lines K) according to reaction 9:

$$Li_2TiO_3 + TiO_2 = Li_2Ti_2O_5 \quad 820-860\ °C \qquad (9)$$

Taking into consideration that there is no detailed information about the crystallographic parameters of $Li_2Ti_2O_5$ in the literature, we synthesized the $Li_2Ti_2O_5$ phase by a solid-state reaction technique and collected XRPD data (Figure 4). The analysis of the X-ray pattern allows us to identify unambiguously the formation of the lithium dititanate, $Li_2Ti_2O_5$.

The diffraction lines of Li_2TiO_3 (line G) and $Li_2Ti_2O_5$ (line K) phases are indiscernible in Figure 2. Therefore, we analyzed the variation of the intensity of the line at $2\theta = 18.5°$ (this line relates to the phase Li_2TiO_3 and/or $Li_2Ti_2O_5$) and the line at $2\theta = 27.5°$ (TiO_2 rutile) as a function of temperature. The intensity of these lines does not vary in the temperature range from 600 to 750 °C. When the temperature is raised from 750 to 850 °C, the intensity of the line at $2\theta = 18.5°$ increases, whereas that of the line at $2\theta = 27.5°$ decreases. This may be accounted for by the fact that in the temperature range from 750 to 850 °C a reaction between the phases Li_2TiO_3 and TiO_2 takes place to form $Li_2Ti_2O_5$.

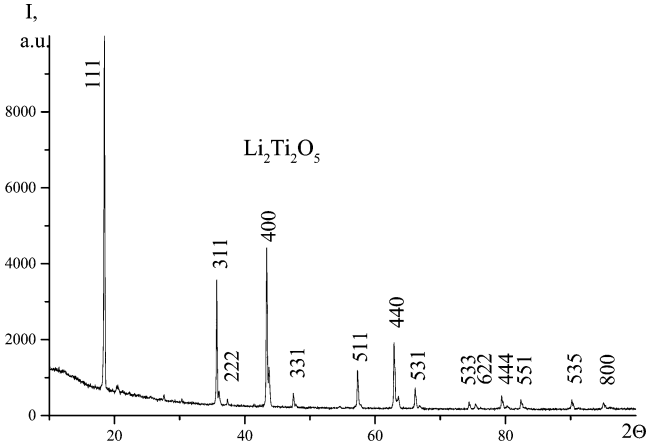

Figure 4. XRPD pattern of $Li_2Ti_2O_5$ prepared by the solid-state reaction technique at 900 °C during 2 h.

At 900 °C the diffraction lines of the perovskite phase P, with starting composition $Li_{0.5}La_{0.5}TiO_3$, appear. At the same temperature, the lithium trititanate $Li_2Ti_3O_7$ also appears as diffraction lines M as well as the lanthanum dititanate $La_2Ti_2O_7$, as diffraction lines L. The diffraction lines of these two last phases increase with temperature up to 1100 °C to finally disappear above this temperature. It is possible to explain these results as follows: the major part of lanthanum oxide, arising from decomposition of $La_2O_2CO_3$, reacts with rutile to form lanthanum dititanate (reaction 10):

$$(1 - {}^{x}/_{2})La_2O_3 + (2 - x)TiO_2 = (1 - {}^{x}/_{2})La_2Ti_2O_7 \quad 850-1100\ °C \qquad (10)$$

The first traces of perovskite-type phase, $Li_{0.5}La_{0.5}TiO_3$, are revealed at 800 °C. Its appearance is described by the following reaction:

$$(1 - x)Li_2Ti_2O_5 + (1 - x)La_2Ti_2O_7 = 4(1 - x)(Li_{0.5}La_{0.5}TiO_3) \quad T > 850\ °C \qquad (11)$$

As temperature increases, part of the lithium dititanate reacts with the remaining titanium oxide to form lithium trititanate:

$$xLi_2Ti_2O_5 + xTiO_2 = xLi_2Ti_3O_7 \quad 900-1100\ °C \qquad (12)$$

XRPD data show that the $Li_2Ti_3O_7$ phase, which forms according to reaction 12, has susceptibility to disproportionate upon interaction with lanthanum oxide to form lithium dititanate and perovskite-like lanthanum lithium titanate, which are more thermodynamically stable:

$$xLi_2Ti_3O_7 + {}^{x}/_{2}La_2O_3 = {}^{x}/_{2}Li_2Ti_2O_5 + 2x(Li_{0.5}La_{0.5}TiO_3) \quad 1000-1100\ °C \qquad (13)$$

(10) Yurchenko, E. N.; Kustova, G. N.; Batsanov, S. S. *Novosibirsk* **1981**, 143 (in Russian).

(11) Ambrogiy, M. A.; Luchnikova, E. F.; Suvorova, M. N. *J. Inorg. Chem.* **1960**, *5*, 366 (in Russian).

Scheme 1. Scheme of $Li_{0.5}La_{0.5}TiO_3$ Synthesis by the Solid−State Reaction Technique

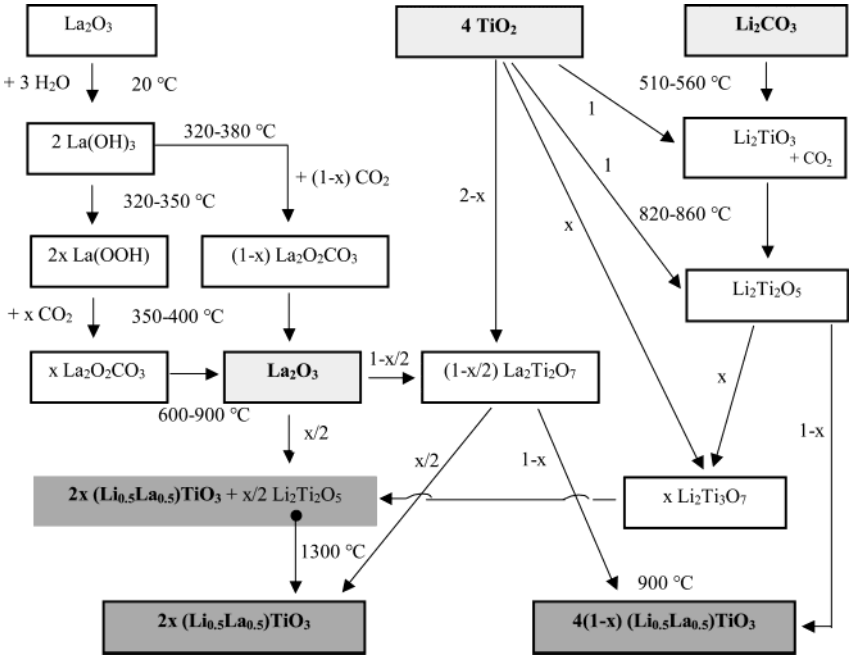

Table 1. Chemical Transformations and Reactions during the Synthesis of $Li_{0.5}La_{0.5}TiO_3$ by the Solid-State Reaction Technique as a Function of Temperature

no.	*t* (°C)	composition	reaction
1	20	Li_2CO_3, TiO_2, $La(OH)_3$	$La_2O_3 + 2H_2O \xrightarrow{20\ °C} 2La(OH)_3$
2	330	Li_2CO_3, TiO_2, $La(OH)_3$, LaOOH	$2xLa(OH)_3 \xrightarrow{320-350\ °C} 2xLaOOH + 2xH_2O\uparrow$
3	360	Li_2CO_3, TiO_2, LaOOH, $La_2O_2CO_3$	$2(1-x)\ La(OH)_3 + (1-x)\ CO_2 \xrightarrow{320-380\ °C} (1-x)La_2O_2CO_3 + 3(1-x)\ H_2O\uparrow$
4	380	Li_2CO_3, TiO_2, $La_2O_2CO_3$	$2xLaOOH + xCO_2 \xrightarrow{350-400\ °C} xLa_2O_2CO_3 + xH_2O\uparrow$
5	530	TiO_2, Li_2TiO_3, $La_2O_2CO_3$	$Li_2CO_3 + TiO_2 \xrightarrow{510-560\ °C} Li_2TiO_3 + CO_2\uparrow$
6	650	TiO_2, Li_2TiO_3, La_2O_3	$La_2O_2CO_3 \xrightarrow{600-900\ °C} La_2O_3 + CO_2\uparrow$ ($La_2O_2CO_3$ decomposed in two stages)
7	840	TiO_2, $Li_2Ti_2O_5$, La_2O_3, $La_2Ti_2O_7$	$Li_2TiO_3 + TiO_2 \xrightarrow{820-860\ °C} Li_2Ti_2O_5$ $(1-{}^{x}/_{2})La_2O_3 + (2-x)TiO_2 \xrightarrow{840-900\ °C} (1-{}^{x}/_{2})La_2Ti_2O_7$
8	900	TiO_2, La_2O_3, $(Li_{0.5}La_{0.5})TiO_3$, $Li_2Ti_2O_5$, $Li_2Ti_3O_7$, $La_2Ti_2O_7$	(a) $xTiO_2 + xLi_2Ti_2O_5 \rightarrow xLi_2Ti_3O_7$ (b) $(1-x)Li_2Ti_2O_5 + (1-x)La_2Ti_2O_7 \rightarrow 4(1-x)(Li_{0.5}La_{0.5})TiO_3$
9	1100	$Li_2Ti_2O_5$, $(Li_{0.5}La_{0.5})TiO_3$, $La_2Ti_2O_7$	${}^{x}/_{2}La_2O_3 + xLi_2Ti_3O_7 \rightarrow 2x(Li_{0.5}La_{0.5})TiO_3 + {}^{x}/_{2}Li_2Ti_2O_5$
10	1300	$(Li_{0.5}La_{0.5})TiO_3$	${}^{x}/_{2}La_2Ti_2O_7 + {}^{x}/_{2}Li_2Ti_2O_5 \xrightarrow{900-1150\ °C} 2x(Li_{0.5}La_{0.5})TiO_3$

Finally the formation of the single-phase perovskite occurs above 1150 °C according to reaction 11 by reaction of $Li_2Ti_2O_5$ formed during reaction 13 and the remaining $La_2Ti_2O_7$ formed according to reaction 11.

The phase content of the mixture after heat treatment at various temperatures and the different chemical reactions and their sequence are shown schematically in Scheme 1 and Table 1. From Scheme 1 we can conclude that the formation of the perovskite-like phase, $Li_{0.5}La_{0.5}TiO_3$, goes through three steps as the temperature increases. Below 1000 °C, the phase $Li_{0.5}La_{0.5}TiO_3$ appears as a result of partial interaction of the phases $Li_2Ti_2O_5$ and $La_2Ti_2O_7$ (reaction 11). An increase of temperature above 1100 °C leads to the formation of the $Li_{0.5}La_{0.5}TiO_3$ phase as a result of interaction of the phases La_2O_3 and $Li_2Ti_3O_7$ (reaction 13). The final formation of the pure perovskite phase $Li_{0.5}La_{0.5}TiO_3$ takes place at a temperature above 1200 °C as a result of the reaction between the phase $La_2Ti_2O_7$, which formed by reaction 10 and is not wholly consumed by

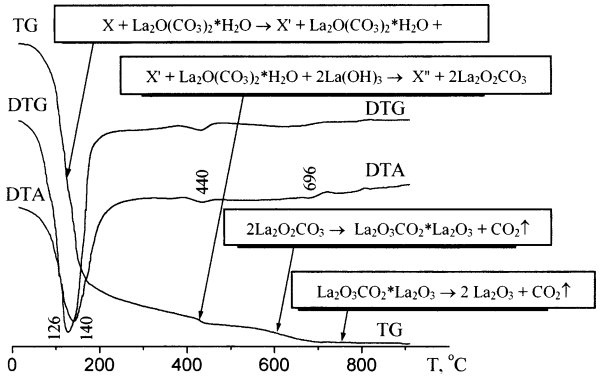

Figure 5. Results of thermal analyses of $Li_{0.5}La_{0.5}TiO_3$ samples prepared by precipitation from solutions.

reaction 11, and $Li_2Ti_2O_5$, which formed by reaction 13:

$$^{x}/_{2}Li_2Ti_2O_5 + {}^{x}/_{2}La_2Ti_2O_7 = 2xLi_{0.5}La_{0.5}TiO_3 \quad (14)$$

(B) Phase Transformation Occurring during Preparation of Ceramics by Precipitation from Solutions. It is known that during synthesis from solutions an insoluble (hard-soluble) precipitate appears in which metals must be in the definite ratio[12] (in our case La:Li:Ti = 1:1:2). Usually, the reagents interact during precipitation to form compounds with definite structure, which we will designate as "inorganic polymer". Formation of the definite structure of "inorganic polymer" facilitates the formation of the final phase under more "soft" conditions as compared with the solid-state reaction technique.[12] It is difficult to define the structure and the chemical composition of such a phase; therefore, it will be designated as phase X. In our case "inorganic polymer" contains hydrated forms of oxyhydroxititanate and lanthanum, which are X-ray-amorphous at room temperature. After precipitation of the "inorganic polymer" lithium carbonate is added.

Figure 5 shows the TG, DTG, and DTA curves of the powders synthesized by precipitation from solutions after addition of lithium carbonate into the precipitate. DTA shows an endothermic process at 120−140 °C, which is accompanied by a considerable loss of weight, as shown by the DTG curve. Figure 6 shows the XRPD patterns and Figure 7 the IR spectra of the final precipitate as a function of heat-treatment temperature in the temperature range from 20 to 1300 °C. Both XRPD patterns and IR spectra are recorded at room temperature.

The XRPD pattern of the final precipitate, dried at 20 °C, shows the diffraction lines of $La_2O(CO_3)_2 \cdot H_2O$. Up to 200 °C, the weight loss, shown in Figure 5, can be attributed to water extraction without any substantial rearrangement of the lattice precipitate. As a result of water loss, the X-ray-amorphous phase X transforms to another X-ray-amorphous phase that we will designate as phase X′. XRPD and IR spectroscopy confirm this transformation. Diffraction lines of lithium carbonate and titanium compounds are absent in the XRPD patterns. Bands in IR spectra at 900 and 1500 cm^{-1} (Figure 7, t = 20 °C) indicate the presence of carbonate groups. In the IR spectra (Figure 7), bands at 865 cm^{-1} (related to the deformation vibrations of CO) and at 1390 cm^{-1} (related to the valence vibrations of CO) weaken as the temperature increases and disappear above 520 °C. This is due to the transformation of $La_2O(CO_3)_2 \cdot H_2O$ into $La_2O_2CO_3$, which is accompanied by degeneration of two valence vibrations to one at 1475 cm^{-1}. The endothermic process at 440 °C, which is accompanied by an insignificant loss of weight, indicates the dehydration of amorphous phase X′ and its transition into a new amorphous phase that we will designate as X″. IR spectra and XRPD patterns do not change substantially with temperature up to 520 °C. The band at 1670 cm^{-1} (δ_s H_2O) in the IR spectra disappears above this temperature, confirming the water extraction. The wide band at 300−800 cm^{-1} is characteristic of the formation of amorphous precipitate.[12] XRPD patterns show the formation of the phases $La(OH)_3$ (diffraction lines A) and $La_2(CO_3)_3 \cdot H_2O$ (diffraction lines N). At 520 °C, the XRPD pattern shows the formation of lanthanum oxycarbonate, $La_2O_2CO_3$ (Figure 6, diffraction lines E).

A further increase of temperature above 680 °C results in the formation of intermediate phases Li_2TiO_3, $Li_2Ti_2O_5$, $La_2Ti_2O_7$, and perovskite phase. The final single-phase product forms in the temperature range from 1000 to 1150 °C as a result of the interaction of $Li_2Ti_2O_5$ and $La_2Ti_2O_7$.

A characteristic feature of thermal curves of the samples obtained by precipitation from solutions, to form perovskite with composition $Li_{0.5}La_{0.5}TiO_3$, is the absence of considerable losses of weight in the temperature range from 600 to 900 °C, in contrast to what is observed for the solid-state reaction technique. Furthermore, the results of comparative analysis of IR spectra (Figures 3 and 7) show that the amount of lanthanum oxycarbonate appearing is insignificant when using the precipitation technique as compared with the solid-state reaction technique. This leads to very small weight losses during decomposition of lanthanum oxycarbonate in the temperature range from 600 to 900 °C.[11] Another difference between these two techniques is the appearance of the perovskite-type phase, $Li_{0.5}La_{0.5}TiO_3$, at lower temperature when the precipitation from solutions technique is used (i.e. 680 °C for precipitation and 900 °C for solid-state reaction).

Scheme 2 and Table 2 show the scheme of perovskite formation in the case of precipitation from solutions and the phase composition after thermal treatment at various temperatures, respectively. Investigations showed that in this case the formation of the perovskite phase, $Li_{0.5}La_{0.5}TiO_3$, occurs under "softer" conditions and at lower temperature than compared with the solid-state reaction technique.

(C) Morphology of the Powders Obtained by Precipitation from Solutions before and after Thermal Treatments at Various Temperatures. The microstructure of the $Li_{0.5}La_{0.5}TiO_3$ powders synthesized by precipitation from solutions before and after thermal treatments at various temperatures is presented in Figure 8 (gain × 10^5). In the temperature range from 20 to 200 °C (Figure 8a,b) powders form agglomerates. However, the grain size is small and does not exceed 5 nm. As the temperature increases, the grain size considerably increases and reaches ca. 70 nm at 460 °C (Figure 8c). A further

(12) Vasserman, I. M. *Chemistry (Leningrad)* **1980**, 207 (in Russian).

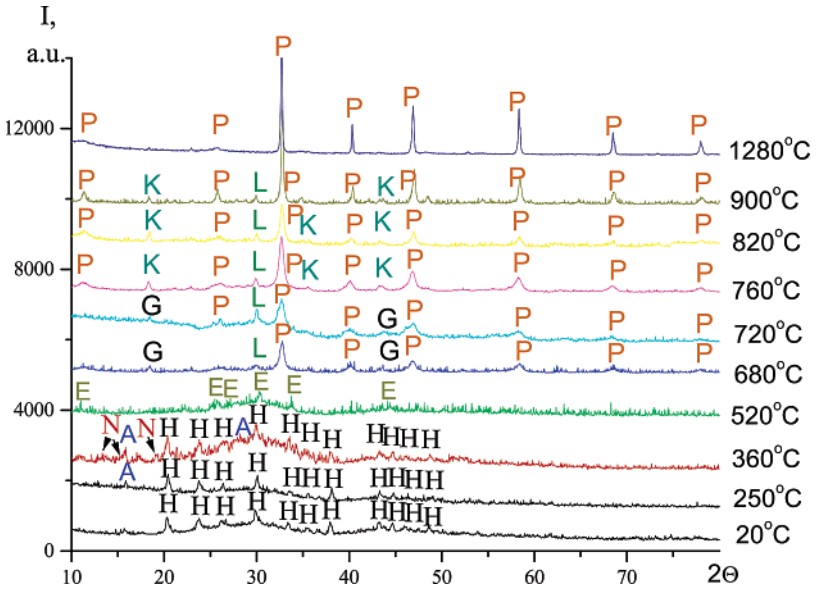

Figure 6. XRPD patterns, obtained at room temperature, of $Li_{0.5}La_{0.5}TiO_3$ samples prepared by precipitation from solutions after heat treatment at different temperature. A = $La(OH)_3$ (36−1421 au); E = $La_2O_2CO_3$ (37−804 au); G = Li_2TiO_3 (33−831 au); H = $La_2O(CO_3)_2 \cdot H_2O$ (28−512 au); K = $Li_2Ti_2O_5$ (38−270 au); L = $La_2Ti_2O_7$ (28−517 au); N = $La_2(CO_3)_3 \cdot H_2O$ (25−1400 au); P = perovskite LLTO.

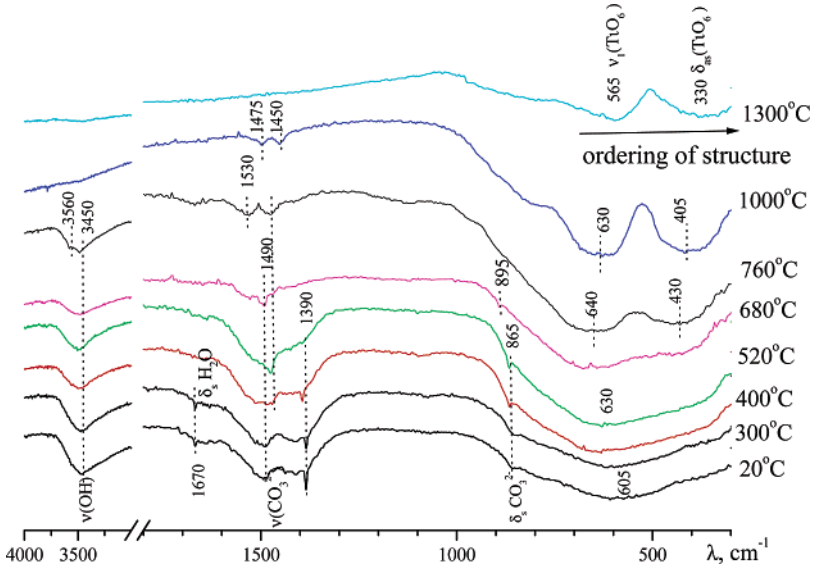

Figure 7. IR spectra of $Li_{0.5}La_{0.5}TiO_3$ powder samples prepared by precipitation from solutions after heat treatment at different temperatures.

increase of temperature results in a sharp decrease of grain size (25−30 nm at 680 °C) (Figure 8d). It should be noted that in the temperature range from 20 to 500 °C, where considerable grain growth is observed, the powders are mostly X-ray amorphous. A considerable loss of weight is also observed due to extraction of free and bounded water. Therefore, in the temperature range from 20 to 500 °C, there is an increase in the size of the grains that are formed during precipitation, and they have the structure of "inorganic polymer" mainly formed of titanium and lanthanum oxyhydroxydes.

Above 500 °C, the structure of the "inorganic polymer" collapses. It is accompanied by a considerable decrease of grain size (25−30 nm at 680 °C) and by the appearance of crystalline phases, including the perovskite one, $Li_{0.5}La_{0.5}TiO_3$. A further increase of temperature (above 700 °C) results in the increase of the grain sizes of the basic phase, $Li_{0.5}La_{0.5}TiO_3$, which reaches ca. 100 nm at 900 °C (Figure 8f). Figure 9 shows the variation of the powder's grain size as a function of heat-treatment temperature.

(D) Chemical Analysis. Results of chemical analysis of polycrystalline powders of the perovskite phase showed that there is substantial loss of lithium from samples. So, chemical analysis of samples synthesized by the solid-state reaction technique and by precipitation from solutions shows that the real composition is $Li_{0.41}La_{0.5}TiO_{2.955}$ for both ceramics after high-temperature sintering.

(E) Electrophysical Properties of the Ceramics. Figure 10a shows the variation of bulk and grain boundary dc conductivity as a function of temperature, plotted in an Arrhenius fashion, in the temperature range from 135 to 550 K, for ceramics prepared by both techniques. These conductivities have been determined by fitting the experimental impedance spectra with the electrical

Table 2. Chemical Transformations and Reactions during the Synthesis of $Li_{0.5}La_{0.5}TiO_3$ by Precipitation from Solutions

no.	*t* (°C)	composition	reaction
1	20	X,[a] $La_2O(CO_3)_2 \cdot H_2O$	
2	200	X′, $La_2O(CO_3)_2 \cdot H_2O$, $La(OH)_3$	X loses water, forming phase X′, which is also amorphous
3	520	X″, $La_2O_2CO_3$	X′ loses water, forming amorphous phase X″
4	680	X″, $La_2Ti_2O_7$, Li_2TiO_3, $(Li_{0.5}La_{0.5})TiO_3$	"inorganic polymer" collapses, forming crystalline phases
5	820	$Li_2Ti_2O_5$, $La_2Ti_2O_7$, $(Li_{0.5}La_{0.5})TiO_3$	perovskite phase appears as a result of the interaction of $Li_2Ti_2O_5$ and $La_2Ti_2O_7$: $Li_2Ti_2O_5 + La_2Ti_2O_7 \rightarrow 4(Li_{0.5}La_{0.5})TiO_3$
6	900	$(Li_{0.5}La_{0.5})TiO_3$, $Li_2Ti_2O_5$, $La_2Ti_2O_7$	
7	1280	$(Li_{0.5}La_{0.5})TiO_3$	

[a] X is an amorphous precipitate, which in the literature is designated as "inorganic polymer".

Scheme 2. Scheme of $(Li_{0.5}La_{0.5})TiO_3$ Synthesis by Precipitation from Solutions[a]

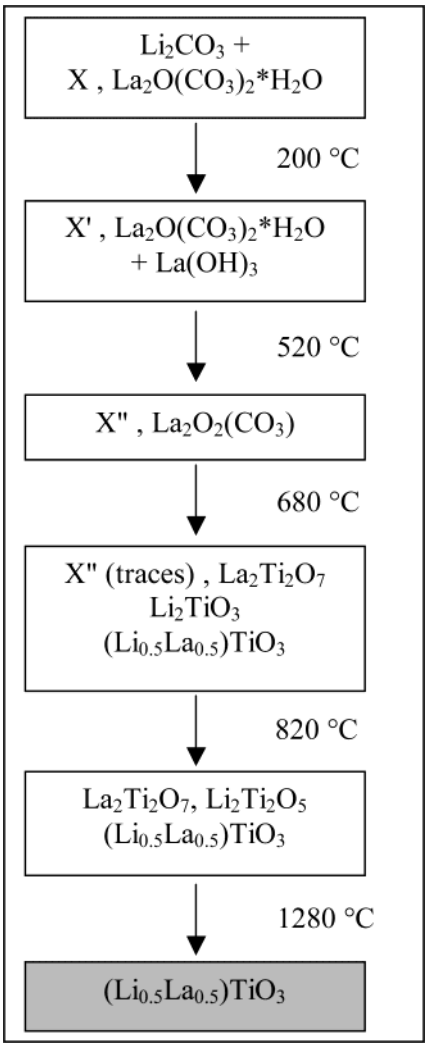

[a] The structure of amorphous phases X, X′, X″ are unknown.

model shown in Figure 10b. Among many possible models, this particular model was able to fit all our experimental impedance diagrams in the large range of temperature investigated.

As described in previous papers, this model is built from the following considerations: (i) the sample is made of both a conductive system (I) and a dielectric one (II). The dielectric system is made of the permanent dipoles of the material, which do not change with motion of ions, and the conductive system is made of the conductive pathways into which the mobile ions travel. (ii) During their motion in the oxide, the mobile ions travel from one electrode to the other successively through the grains and through the grain boundaries. (iii) Both systems, dielectric and conductive, respond to the ac applied voltage. According to these considerations, we used an electrical model with ZARC elements. The dielectric part of our sample is represented by a constant phase element (CPE1), and the conductive part is represented by two ZARC elements, ZARC2 (R_2, CPE2) for bulk and ZARC3 (R_3, CPE3) for grain boundary. Finally, the electrode part of the sample is represented by a constant phase element (CPE4). The inductance of wires is represented by the L element. As suggested by Macdonald,[13] this model (named circuit O in the LEVMW software[14]) is useful for fitting dielectric and high-resistivity data associated with mobile ions, as is the case with LLTO at low temperature. At high temperature, the dielectric part has a very small influence (even none) on the impedance data. We recall that we take the following model for the impedance of the CPE distributed element

$$Z_{CPE} = 1/[A(j\omega)^n]$$

where A is the frequency-independent real constant, $j = \sqrt{-1}$, ω is the angular frequency, and n ($0 < n < 1$) is the constant phase parameter that is linked to the constant phase angle φ through the relationship $\varphi = 2\pi n$.

From the fitted parameters R_2 and R_3, it is possible to determine the bulk and grain boundary conductivity. The frequency-independent real constant A_2 of CPE2 is close to a true capacitance ($n_2 \approx 1$), its magnitude being on the order of 10^{-11} F; the A_3 component of CPE3 is not a true capacitance ($n_3 \approx 0.8-0.9$), its magnitude being on the order of 10^{-8} F s^{n_3}. These two different values of A able us to ascribed the ZARC2 element to the impedance of the bulk and the ZARC3 element to the grain boundary one. As observed in Figure 10a, the bulk conductivity does not depend on the preparation techniques. This is not surprising, since both techniques lead to the same oxide phase, as explained above, with therefore the same electrical properties. The bulk σ_{dc} curves display a S-shape, as described previously for this oxide.[5,15] This behavior cannot be ascribed to a structural change in LLTO, since both neutron diffraction performed from RT down to 4 K[16] and high-temperature XRPD patterns obtained on LLTO up to 1470 K,[17] did

(13) Macdonald, J. R. *J. Non-Cryst. Solids* **1997**, *197*, 83.
(14) The latest version of the LEVMW fitting software may be obtained at no cost from the Solartron Instruments website.
(15) Emery, J.; Buzaré, J.-Y.; Bohnké, O.; Fourquet, J.-L. *Solid State Ionics.* **1997**, *99*, 41.
(16) Bohnké, O. ILL report 1996 (unpublished results).

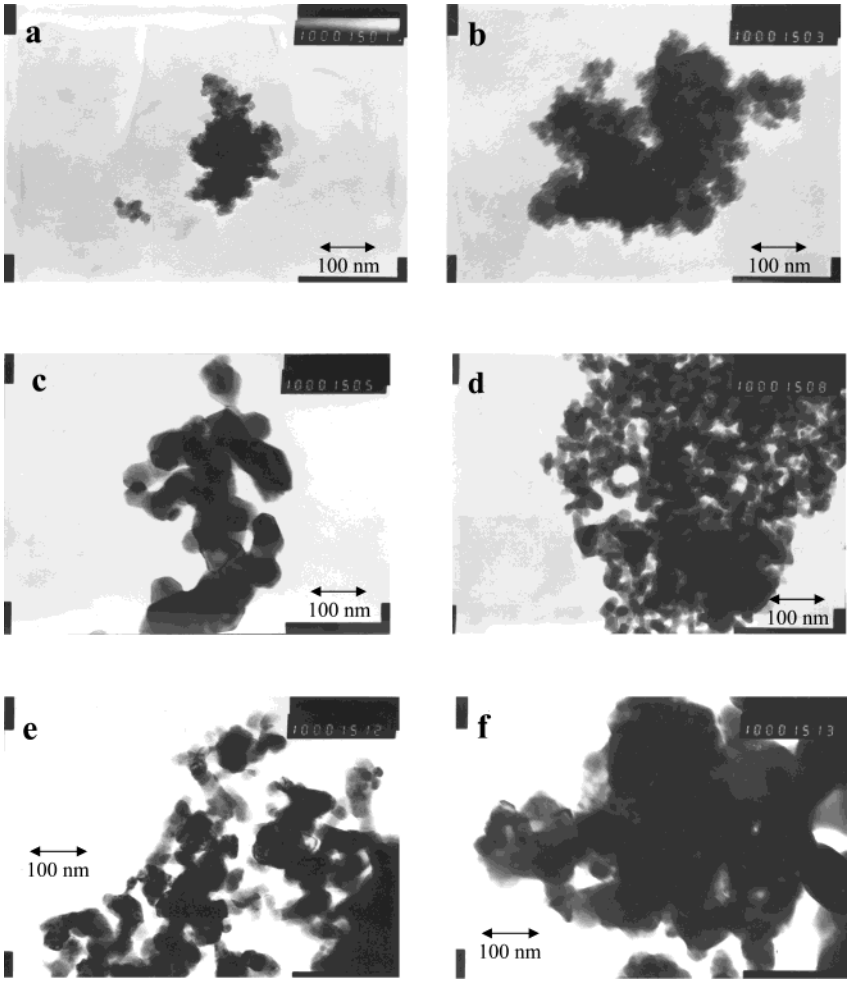

Figure 8. Microstructure of powders of $(Li_{0.5}La_{0.5})TiO_3$ prepared by precipitation from solutions without heat treatment (a) and after heat treatment during 2 h at 200 °C (b), 460 °C (c), 680 °C (d), 780 °C (e), and 900 °C (f).

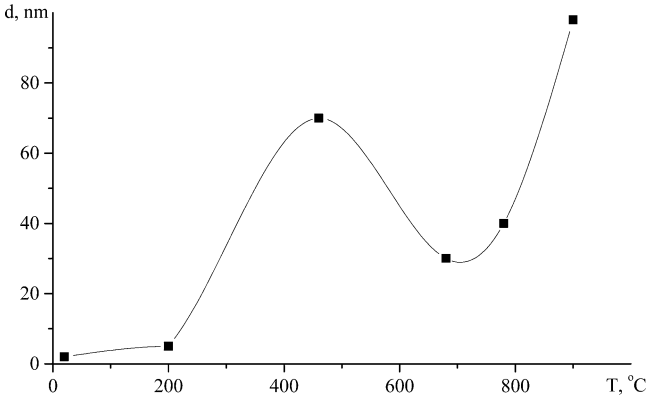

Figure 9. Grain size of $(Li_{0.5}La_{0.5})TiO_3$ powder prepared by precipitation from solutions versus temperature of heat treatment.

not reveal any structural change. A change of conduction mechanism can then be invoked.

Below RT, σ_{dc} follows a classical Arrhenius law expressed as

$$\sigma_{dc} = \frac{\sigma_0}{T}\exp\left(-\frac{E_a}{RT}\right)$$

suggesting that the ionic motion is thermally activated. In the thermally activated temperature domain ($T <$ RT), a change of activation energy is observed at 200 K. Below 200 K, an activation energy $E_a = 0.270 \pm 0.005$ eV and a preexponential factor $\sigma_0 = 5.1 \pm 0.1\ 10^3$ S cm^{-1} K can be determined. As temperature increases above 200 K, the activation energy increases to 0.305 ± 0.005 eV and σ_0 increases 1 order of magnitude to reach $\sigma_0 = 3.9 \pm 0.1\ 10^4$ S cm^{-1} K. The increase of E_a suggests a change in the conduction pathways and the increase of σ_0 suggests that the number of long-range moving ions increases as temperature increases, some Li^+ ions being trapped in the A-cage of the perovskite structure at low temperature.

Above room temperature, the plot displays a concave curvature. This effect can be described by a Vogel−Tamman−Fulcher (VTF)-type relationship, as suggested in a previous paper.[5] Originally, the VTF relationship was developed to deal with viscosity properties of supercooled liquids. It has been extended to charged carrier motion in amorphous materials, such as glasses or polymers[18] This relationship, based on the free volume theory,[19] can be expressed as

$$\sigma_{dc} = AT^{-1/2}\exp\left(-\frac{B}{R(T - T_0)}\right)$$

where A is the prefactor, B a pseudo-activation energy,

(17) Bohnké, O.; Duroy, H.; Fourquet, J.-L.; Ronchetti, S.; Mazza, D. *Solid State Ionics* **2002**, *149*, 1−2, 81.

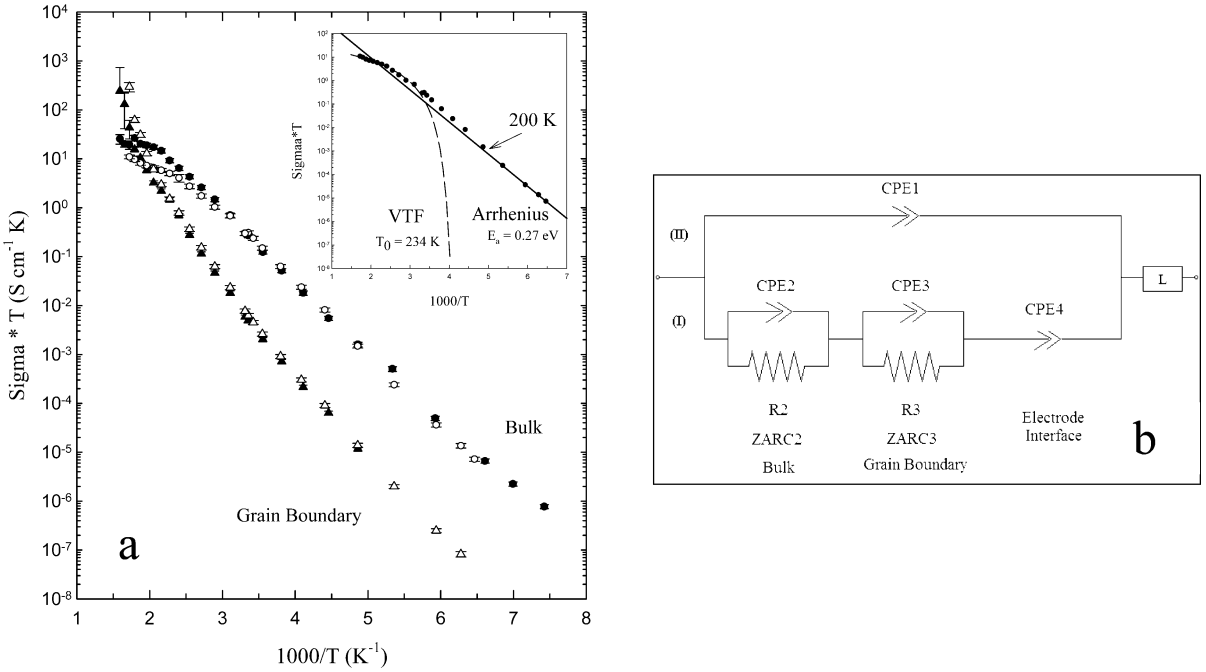

Figure 10. (a) Arrhenius plots of the bulk and grain boundary dc conductivity of $(Li_{0.5}La_{0.5})TiO_3$ ceramics obtained by solid-state reaction techniques (white symbols) and precipitation from solutions (black symbols). The two mechanisms of conduction, Arrhenius and VTF, are shown in the inset of the figure for the ceramic obtained by the solid-state reaction technique. The same behavior is observed for ceramic obtained by precipitation. (b) Electrical model used for the fitting of the experimental data.

and T_0 a characteristic temperature, the temperature at which the free volume becomes zero.[20] Such a conduction mechanism is thermally assisted, which means that the conducting process is largely promoted by the polymer chain movement and also that the distribution of barriers between the sites is constantly changing with time due to the chain movement. We could postulate that in these crystalline oxides a distribution of activation energy between the sites occurs and also that it is changing with time due to the lattice vibrations. However much work remains to be done to clarify this point and to explain the concave curvature of the conductivity vs reciprocal temperature plot in disordered crystalline materials. The fitting of the experimental data with the above VTF relationship leads to $A = 0.98$ S cm^{-1} K$^{1/2}$, $B = 0.03$ eV, and $T_0 = 234$ K for LLTO obtained by the solid-state reaction technique and to $A = 4.26$ S cm^{-1} K$^{1/2}$, $B = 0.04$ eV, and $T_0 = 244$ K for LLTO obtained by the precipitation technique. The dashed line in the inset represents the VTF relationship calculated with the above parameters. These two mechanisms, which occur in the grains of the oxide, are independent of the method of preparation of the oxide, as soon as the synthesis leads to the same material. Therefore the same bulk conductivity is observed.

A more surprising result is the identical value of the grain boundary conductivity observed for both ceramics. As previously explained, the two preparation techniques lead to powders of different grain size. It has been shown previously that nanosized grains can be obtained by precipitation from solutions. However the heat treatment of the titanate powder obtained by this method influences the grain size. At 900 °C, the grain size is around 0.1 μm. After sintering at 1280 °C for 2 h SEM pictures show that the grain size increases up to 2−5 μm (Figure 11b). This is also the grain size of the ceramics obtained by the solid-state reaction technique (Figure 11a). Therefore, the similar grain boundary conductivity, observed in Figure 10, can be explained by the final high-temperature sintering of the prepared powders. The similar grain size explains the results of conductivity. This result shows clearly that to take advantage of the grain size of a material, and of properties accompanying this grain size, it is necessary to take care of the sintering temperature.

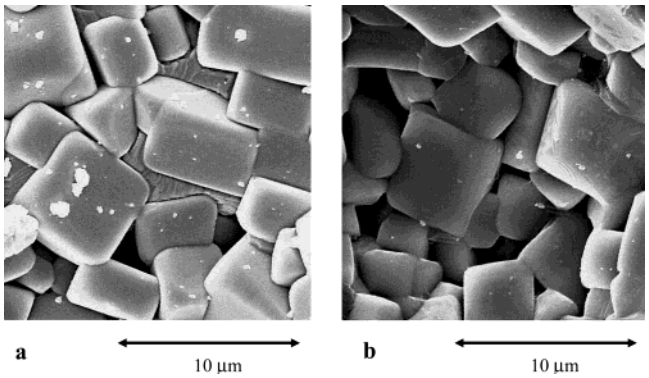

Figure 11. SEM images of $(Li_{0.5}La_{0.5})TiO_3$ ceramics obtained by solid-state reaction (a) and precipitation from solutions (b) after sintering for 2 h at 1300 °C and 1280 °C, respectively.

Further studies are on the way to prepare ceramics with small grain sizes. Experiments of dilatometry will be carried out on these powders, and sintering at temperature between 900 and 1280 °C will be performed on very fine grain LLTO obtained by precipitation to avoid the increase of the grains.

(18) Ratner M. A. *Polym. Electrolytes Rev.* **1987**, *1*, 173.
(19) Vogel, H. *Phys. Z.* **1921**, *22*, 645; Tamman, G.; Heese, W. Z. *Anorg. Chem.* **1926**, *156*, 245. Fulcher, G. S. *J. Am. Ceram. Soc.* **1925**, *8*, 339.
(20) Cohen, M. H.; Turnbull, D. *J. Chem. Phys.* **1959**, *31*, 1164.

Conclusions

As a result of the investigations carried out, the phase transformations and the successive chemical reactions occurring during the synthesis of lanthanum lithium titanate, $Li_{0.5}La_{0.5}TiO_3$, with perovskite-like structure, either by the solid-state reaction technique or by precipitation from solutions are described. It is shown that this is a multistage process. The chemical analysis showed that the lithium loss occurs during the synthesis and that the synthesized ceramics have the chemical composition $Li_{0.41}La_{0.5}TiO_{2.955}$. The perovskite phase obtained by precipitation from solutions is made of nanoparticles of 5 nm size at low temperature. The grain size increases as temperature increases to reach 100 nm at 900 °C. After sintering at high temperature, the ceramics are made of grains of size on the order of 2−5 μm, whatever the technique of synthesis used. Although the titanate obtained by precipitation from solutions is made of a powder of very fine grains, the high-temperature heating increases the grain size, and therefore, this heating leads to ceramics with the same conductivity as those synthesized from the solid-state reaction. Heat treatment at lower temperature than 1280 °C is necessary to keep the advantages of the precipitation technique: formation of nanosized powders of titanate phase and synthesis under milder conditions as compared with the solid-state reaction technique.

CM034820X